Graphite nanosheet-based composites for mediator-free H_2O_2 biosensor

Xu Chen, Chenglin Fu and Wensheng Yang*

Received 2nd June 2009, Accepted 28th July 2009
First published as an Advance Article on the web 19th August 2009
DOI: 10.1039/b910754a

Graphite nanosheet (GNS)–Nafion composites were prepared for the immobilization of hemoglobin (Hb) to construct a mediator-free H_2O_2 biosensor. Scanning electron microscopy (SEM), UV-vis spectroscopy and Fourier transform infrared spectroscopy were used to characterize the Hb–GNS–Nafion composite film. Due to good biocompatibility of the composite film, immobilized Hb retained its native structure. The Hb–GNS–Nafion composite film-modified electrodes showed direct electrochemistry with a fast electron-transfer rate (6.63 s^{-1}) and high electrocatalytic activity to the reduction of hydrogen peroxide (H_2O_2). The resulting biosensor exhibited a high sensitivity of 412.7 mA M^{-1} cm^{-2}, a low detection limit of 2.0×10^{-7} M, and a small apparent Michaelis–Menten constant of 37 μM. These results were comparable or superior to the biosensors based on the carbon nanofiber (CNF)- and carbon nanotube (CNT)-based biosensors. Due to the lower cost of GNSs, the GNS-based composite can combine with other redox proteins and widely apply in mediator-free biosensors, bioelectronics and biofuel cells.

1. Introduction

The use of nanomaterials for the design of biosensors has received much attention in recent years because the unique properties of nanomaterials offer excellent prospects for designing novel sensing systems and enhancing the performance of biosensors.[1–3] Among various nanomaterials, carbon-based nanomaterials have been shown to be ideal for biosensor applications since they are conductive, biocompatible, easily functionalized, and possess very large surface areas.[4,5] They can be used as immobilization matrices for biomolecules, while at the same time they can relay the electrochemical signal, acting as transducers. Of these carbon-based nanomaterials, carbon nanotubes (CNTs) are most widely used in biosensor systems.[6–8] The incorporation of CNTs has greatly increased biosensor sensitivity, expedited response speed and promoted electron-transfer rates. Recently, increasing attention has been paid to the biosensing application of carbon nanofibers (CNFs).[9–12] Due to different stacking manners of carbon orbitals on the surface, CNFs possess less order and more edge sites on the outer wall and thus have a much larger functionalized surface area compared with that of CNTs. Higher sensitivity as well as improved operational and storage stabilities over those prepared with CNTs could be obtained from CNF-based biosensors. In addition, as another member of the carbon family, C_{60} could significantly accelerate direct electron-transfer kinetics of proteins in multiple walled CNT (MWCNT) composite films and has showed potential in biosensing applications.[13] Therefore, the use of different structural carbon-based nanomaterials provides a promising future for the development of excellent biosensors.

Graphite is a naturally abundant layered carbon-based material and consists of superimposed lamellae of two-dimensional carbon–carbon covalent networks, referred to as graphene, which stack along the *c*-axis. Microsized graphite particles as a carbon paste[14] or composite[15,16] have been used in electrochemical sensors for years. However, the biosensors based on these microsized graphite particle electrodes were normally not very sensitive and their response was slow because of their relatively low surface area. Recently, by exfoliating the graphite layers, thin graphite nanosheets (GNSs) have been formed[17,18] which possess high surface area. The theoretical surface area of a graphite sheet is close to 2700 m^2 g^{-1}.[19] Moreover, thin GNSs exhibit intriguing properties such as remarkable electrical conductivity, ultra-high Young's modulus and high thermal conductivity, which make them suitable building blocks in many potential electronic applications[20] or additives for high-performance materials.[21–23] As a promising and excellent carbon-based nanomaterial, the application of GNSs in bioelectronics and biosensors has been rarely explored.[24–27]

The objective of this work was to explore the ability of GNSs in promoting direct electron transfer between redox proteins and electrodes and to further use GNSs for the development of mediator-free biosensors. Compared with first-generation biosensors (mostly using oxygen as mediator) and second-generation biosensors (using artificial redox mediators), third-generation biosensors based on the direct electron transfer of proteins (*i.e.* mediator-free) have some advantages,[28] such as the absence of the influence of oxygen concentration and the poisoning of biomolecules owing to the introduction of artificial mediators, more simplification for the fabrication of biosensors and so on. More importantly, the absence of mediators can lead to a superior selectivity because the operating potential of the biosensors bases on direct electron transfer is closer to the redox potential of the enzyme[29,30] and they are therefore less prone to interfering reactions.[31] However, for the development of third-generation biosensors, a critical challenge to the successful realization of direct electron transfer between redox proteins and electrodes must be overcome.

State Key Laboratory of Chemical Resource Engineering, Beijing University of Chemical Technology, Beijing 100029, P R China. E-mail: yangws@mail.buct.edu.cn; Fax: +86 10 64425385; Tel: +86 10 64435271

In this paper, hemoglobin (Hb) was selected as a model redox protein. Nafion was employed as an effective solubilizing agent[24,32] for GNSs to form a GNS–Nafion composite for the immobilization of biomolecules. The direct electrochemistry of Hb immobilized in the GNS–Nafion composite film was studied. The potential application of the protein electrode as a mediator-free biosensor for the detection of hydrogen peroxide (H_2O_2) was explored.

2. Experimental

2.1. Materials

Graphite nanosheets were donated by Prof. Chen (Huaqiao University, China), which were synthesized and characterized according to their previously reported method.[17] Hemoglobin (from bovine blood) and Nafion (5 wt% in lower aliphatic alcohols and water mixture) were purchased from Sigma. All other reagents were of analytical grade. Phosphate buffer solutions (PBS) with various pH values were prepared by mixing the stock standard solutions of Na_2HPO_4 and NaH_2PO_4. All aqueous solutions were prepared with deionized, doubly distilled water.

2.2. Preparation of film electrodes

To obtain good cyclic voltammetric response and stability of the biosensor, the concentrations and mass ratios of Nafion, GNSs and Hb in the Hb–GNS–Nafion mixture were optimized in control experiments. Herein, a mixture containing 0.85 wt% Nafion, 0.17 wt% GNSs and 0.3 wt% Hb was selected as the optimal fabrication parameters for the preparation of the biosensor.

Prior to use, glassy carbon electrodes (GCEs, diameter 3 mm) were first polished with 1.0, 0.3, and 0.05 μm alumina powder, respectively, rinsed thoroughly with doubly distilled water between each polishing step, and then sonicated in doubly distilled water and dried with a purified nitrogen stream. The film electrode was prepared by a simple casting method. Firstly, a 1 wt% Nafion solution was prepared by diluting the 5 wt% Nafion stock solution with a water–alcohol (65% alcohol, v/v) solution. Secondly, a 0.2 wt% GNS–Nafion suspension was obtained by adding GNSs into the 1 wt% Nafion solution by the aid of ultrasonication and stirring. Then an Hb–GNS–Nafion suspension was prepared by mixing 85 μL of the GNS–Nafion suspension with 15 μL of an Hb solution (20 mg mL^{-1}, dissolved in 0.05 M pH 7.0 PBS) and sonicating for 5 min. Finally, 4 μL of the Hb–GNS–Nafion suspension was cast onto the surface of a clean GCE and dried at room temperature to prepare the Hb–GNS–Nafion/GCE. For comparison, the Hb/GC and Hb–Nafion/GC electrodes were also prepared according to the same procedure. Prior to electrochemical experiments, the modified electrodes were rinsed thoroughly with doubly distilled water and kept in 0.05 M pH 7.0 PBS at 4 °C when not in use.

2.3. Electrochemical measurements

Electrochemical measurements were carried out on a CHI 660B electrochemical workstation (Shanghai Chenhua Instrument Co., China). A conventional three-electrode system was used with the as-prepared film electrode as the working electrode, a platinum wire as the auxiliary electrode, and a saturated Ag/AgCl electrode as the reference electrode. All experimental solutions were deoxygenated by bubbling highly purified nitrogen for 20 min and a nitrogen atmosphere was maintained during electrochemical measurements. All measurements were performed at room temperature.

2.4. Spectroscopic analysis and morphological characterization

UV-vis experiments were performed with a Shimadzu UV-2501 PC spectrophotometer. Circular dichroism (CD) measurements were carried out on a Jasco J-1200 spectropolarimeter. Fourier transform infrared (FTIR) spectra were recorded on a Bruker Vector 22 FTIR spectrometer. Field emission scanning electron microscopy (FESEM) images were obtained with an Hitachi S4700 scanning electron microscope at an accelerating voltage of 20 kV.

3. Results and discussion

3.1. Morphological characterization of GNSs and Hb–GNS–Nafion composite film

Fig. 1A shows the SEM image of the GNSs. As seen from Fig. 1A, GNSs have sheet-like structures with the diameter ranging from 0.2 to 2 μm. The thickness of the GNSs is estimated about 10–50 nm from the inset of Fig. 1A. Fig. 1B shows the SEM image of the Hb–GNS–Nafion composite film. It can be seen that GNSs were uniformly embedded in Nafion to form a stable composite film, which was essential for the stability of the prepared enzyme electrode.[12] Most of nanosheets in the

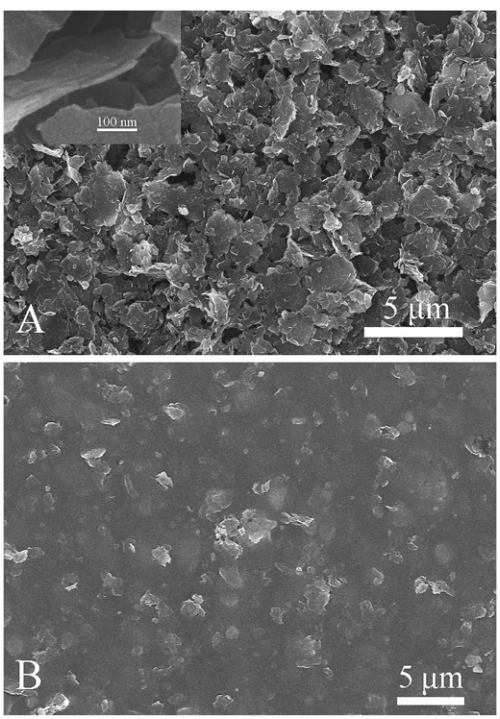

Fig. 1 SEM images of GNSs (A) and Hb–GNS–Nafion composite film (B). Inset in Fig. 1A: a high magnification SEM of GNSs.

composite film were laying flat. However some edges of sheets were sticking out of the surface, which makes a relatively rough surface. This rough surface is generally beneficial in increasing the sensitivity of an amperometric electrode.[24]

3.2. Spectroscopic characterization of Hb–GNS–Nafion composite film

Hb immobilized in the GNS–Nafion composite film was investigated by spectroscopic analysis. UV-vis spectrometry is an effective technique to probe the characteristic structure of proteins. The position of the Soret absorption band of heme can provide some information about the denaturation of heme proteins and conformational changes of the heme group region. Fig. 2 shows the UV-vis absorption spectra of Hb and Hb–GNS–Nafion composite film. The Soret band of Hb in the composite film is located at 410 nm, which is nearly the same as the position of a native Hb film of 411.5 nm. This indicated that Hb retained its native structure in the GNS–Nafion composite film. Furthermore, the circular dichroism (CD) spectrum was used to study the conformational information of native Hb solution and Hb–GNS–Nafion diluent suspension solution (data not shown). The native Hb showed double minima at 210 and 222 nm. Similar peaks as native Hb were found in Hb–GNS–Nafion CD spectrum, confirming that most of the secondary structure of Hb in the GNS–Nafion solution was retained.

The IR vibrational bands of the amide group of Hb are also sensitive to the protein secondary structure. The amide I band (1700–1600 cm^{-1}) is attributed to the C=O stretching vibration of peptide linkages in the backbone of the protein. The amide II band (1620–1500 cm^{-1}) results from the combination of N–H bending and C–N stretching. The FTIR spectra of free Hb and immobilized Hb are shown in Fig. 3. The spectra of amide I and II bands of Hb immobilized in the GNS–Nafion composite film (1643 and 1540 cm^{-1}) are at essentially the same positions as those obtained for native Hb (1650 and 1540 cm^{-1}), suggesting that Hb retained the essential features of its native secondary structure in the GNS–Nafion composite film. The slight shift of the amide I band (from 1650 to 1643 cm^{-1}) indicated that there might be some interaction between Hb and the GNS–Nafion matrix. The results of spectroscopic characterization demonstrated that the GNS–Nafion composite film had good biocompatibility.

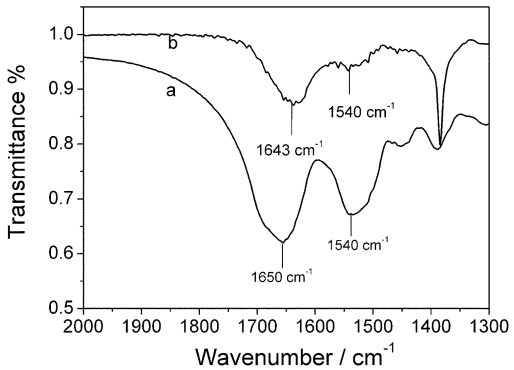

Fig. 3 FTIR spectra of (a) Hb and (b) Hb–GNS–Nafion composite.

3.3. Direct electrochemistry of Hb–GNS–Nafion composite film-modified electrodes

Cyclic voltammetry was used to study the direct electrochemistry of Hb immobilized in the GNS–Nafion composite film. Fig. 4 shows the cyclic voltammograms (CVs) of different electrodes measured in 0.1 M N_2-saturated PBS (pH 7.0) at a scan rate of 0.1 V s^{-1}. No obvious redox peaks were observed at the Hb/GCE (Fig. 4a). However, the Hb–GNS–Nafion/GCE (Fig. 4c) gave a couple of stable and well-defined redox peaks at −0.277 and −0.318 V, corresponding to the Hb–Fe^{III}/Fe^{II} redox couple. Although the Hb–Nafion/GCE also displayed a couple of redox peaks of Hb (Fig. 4b), these peak currents were much smaller than those of the Hb–GNS–Nafion/GCE. This indicated that the introduction of GNSs into films could greatly enhance the direct electron transfer between Hb molecules and GCEs. The formal potential ($E^{o\prime}$) of the heme $Fe^{III/II}$ couple in the Hb–GNS–Nafion/GCE, estimated as the midpoint of reduction and oxidation potentials, was −0.298 V. A small peak potential separation (ΔE_p) of 41 mV between the reduction and oxidation peak potentials was obtained, indicating a fast electron-transfer process.

Fig. 5 shows the CVs of the Hb–GNS–Nafion/GCE at various scan rates. The peak currents increased linearly with scan rates from 0.05 to 0.5 V s^{-1} (the inset of Fig. 5), indicating a surface-controlled electrochemical process. From the peak-to-peak separation of CVs with scan rates from 0.05 to 0.5 V s^{-1}, the

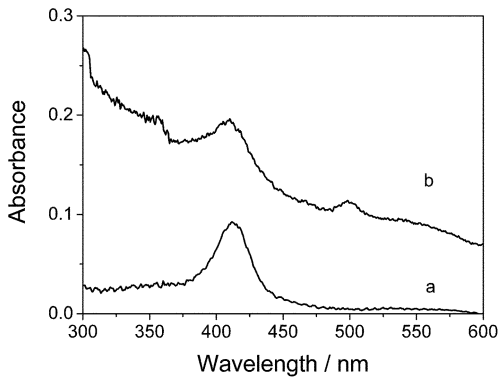

Fig. 2 UV-vis absorption spectra of (a) Hb film and (b) Hb–GNS–Nafion film on quartz glass.

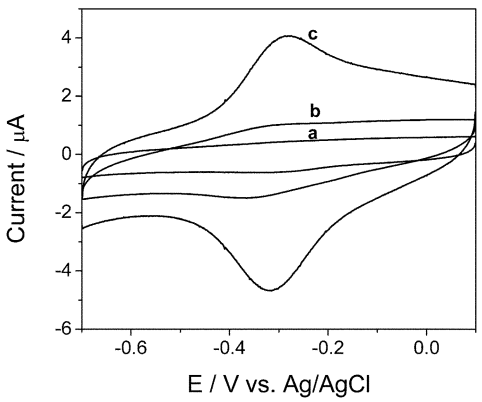

Fig. 4 CVs of (a) Hb/GCE, (b) Hb–Nafion/GCE and (c) Hb–GNS–Nafion/GCE in 0.1 M PBS (pH 7.0). Scan rate, 0.1 V s^{-1}.

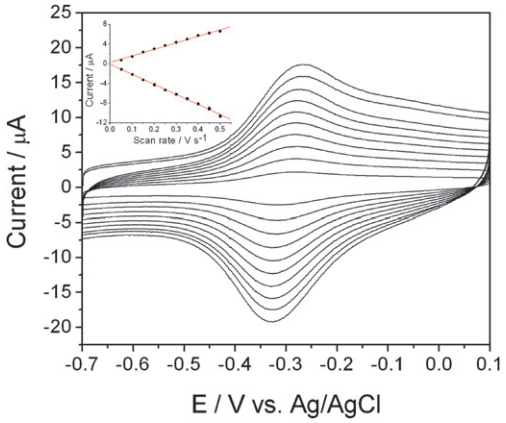

Fig. 5 CVs of Hb–GNS–Nafion/GCE at different scan rates in 0.1 M PBS (pH 7.0). Inset: plots of oxidation and reduction peak currents *versus* scan rate. (From inner to outer CVs: 0.05, 0.10, 0.15, 0.20, 0.25, 0.30, 0.35, 0.40, 0.45 and 0.50 V s^{-1}.)

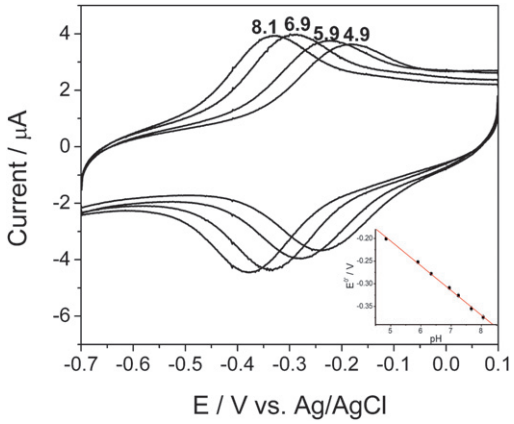

Fig. 6 CVs of Hb–GNS–Nafion/GCE in 0.1 M PBS with various pH values. Inset: plot of formal potential *versus* pH value. Scan rate, 0.1 V s^{-1}.

average electron-transfer rate constant k_s of the Hb immobilized in the composite film was estimated to be 6.63 s^{-1} according to the model of Laviron with the formula $k_s = mnFv/RT$,[33] where n is the number of electrons transferred, F is Faraday's constant, m is a parameter related to the peak-to-peak separation, v is the scan rate, R is the gas constant, and T is the temperature. Here, $T = 298$ K and $n = 1$. This value was more than two times of that of 2.4 s^{-1} for Hb entrapped in a CNF–Nafion composite film,[12] and was more than five times of those for Hb immobilized in CNT-based films (0.062 s^{-1},[34] 0.58 s^{-1},[35] 1.02 s^{-1},[36] and 1.25 s^{-1} [37]) and C_{60}-MWCNT (0.39 s^{-1} [13]), suggesting that the GNS–Nafion composite film was much more effective in facilitating the direct electron transfer of Hb than CNF- and CNT-based films. The faster electron-transfer kinetics in the GNS–Nafion composites was possibly attributed to the abundant edge sites on the GNSs, since a high proportion of edge sites is known to lead to more facile electron transfer.[38] From the integration of the reduction peaks of the Hb–GNS–Nafion/GCE at different scan rates, an average surface coverage of Hb was calculated to be 3.1×10^{-10} mol cm^{-2}, which was comparable to the reported value for the CNF–Nafion composite film,[12] and was much higher than that for the CNT–Nafion film.[37] The percentage of the electroactive Hb on the electrode surface was estimated to be about 18.7%.

In most cases, the redox behavior of proteins is often significantly dependent on the solution pH. The CVs of the Hb–GNS–Nafion/GCE showed a strong dependence on solution pH. Fig. 6 shows the effect of solution pH on the response of the Hb–GNS–Nafion/GCE. With the increase of the solution pH from 4.9 to 8.1, the negative shifts of both reduction and oxidation peak potentials were observed. The plot of the formal potential *versus* pH showed a slope of −54.5 mV pH^{-1} in the inset of Fig. 6. The value was reasonably close to the theoretical value of −59.0 mV pH^{-1} at 25 °C, indicating a reversible, one-proton-coupled single-electron-transfer process.[39] In addition, all changes in voltammetric peak potentials and currents with pH were reversible.

3.4. Biosensor applications

Apparently, the good biocompatibility and abundant edge sites of the GNS–Nafion composite film offer great advantages for the fabrication of a mediator-free biosensor. The determination of H_2O_2 is of great importance in clinical, food, pharmaceutical and environment analyses. The electrocatalytic properties of the Hb–GNS–Nafion/GCE towards H_2O_2 are shown in Fig. 7. When H_2O_2 was added into blank PBS, a significant increase in the reduction peak current at about −0.318 V was observed accompanying a decrease of oxidation peak current, displaying a typical electrocatalytic reduction process of H_2O_2. In addition, the reduction current at around −0.14 V increased with the addition of H_2O_2, which was possibly due to the electrocatalysis of GNSs to the reduction of H_2O_2.[24,25]

The Hb–GNS–Nafion/GCE employed as a mediator-free biosensor for the detection of H_2O_2 was further investigated by amperometry. The current was monitored at a constant potential of −0.33 V while aliquots of H_2O_2 were injected in to the pH 7.0 PBS. Fig. 8 shows the calibration curve of the H_2O_2 biosensor, and the inset picture of Fig. 8 shows typical current–time plots for GNS–Nafion/GCE (a) and Hb–GNS–Nafion/GCE (b) on successive injections of various concentrations of H_2O_2 solution at −0.33 V. In the absence of biocatalytic activity (Fig. 8a), the increase of the electrocatalytic current was much smaller with successive additions of 2 μM H_2O_2. In contrast, the Hb–GNS–Nafion/GCE responded more sensitively to the

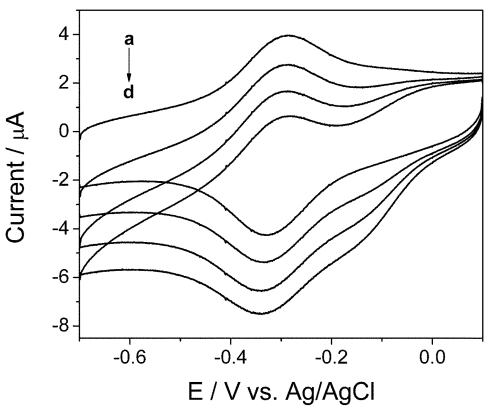

Fig. 7 CVs of Hb–GNS–Nafion/GCE in 0.1 M PBS (pH 7.0) containing (a) 0, (b) 100, (c) 200, and (d) 300 μM H_2O_2. Scan rate, 0.1 V s^{-1}.

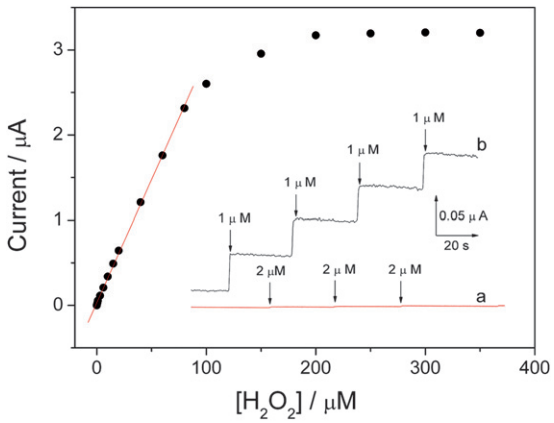

Fig. 8 Calibration curve of the biosensor as a function of H_2O_2 concentration. The inset shows typical current–time plots for GNS–Nafion/GCE (a) and Hb–GNS–Nafion/GCE (b) on successive injections of various concentrations of H_2O_2 solution. Applied potential, −0.33 V *vs.* Ag/AgCl.

change in the substrate concentration. Thus, the catalytic response of GNSs to the reduction of H_2O_2 can be omitted. The response time (achieving 95% of the steady-state current) of the biosensor was less than 5 s, indicating a very fast response to H_2O_2. The linear range of the biosensor is from 5.0×10^{-7} to 8.0×10^{-5} M with a correlation coefficient of 0.9995 ($n = 16$). The Hb–GNS–Nafion/GCE showed a sensitivity of 412.7 mA M^{-1} cm^{-2} and a detection limit of 2.0×10^{-7} M (S/N = 3) for H_2O_2. Compared with Hb entrapped in the CNF–Nafion film,[12] the Hb–GNS–Nafion/GCE had a wider linear detection range and higher sensitivity. The detection limit was much lower than previously reported CNT-based biosensors.[34,35,37] These good properties were also observed with the recently reported graphene-based/GCE,[26,27] indicating that thin GNSs hold great promise for biosensing applications.

When the concentration of H_2O_2 was higher than 150 μM, the catalytic current tended to level off, suggesting a typical Michaelis–Menten process. The apparent Michaelis–Menten constant (K_M^{app}), a reflection of both the enzymatic affinity and the ratio of microscopic kinetic constants, was obtained from the electrochemical version of the Lineweaver–Burk equation[40] to be 37 μM. This value was much smaller than those of Hb entrapped in the CNF–Nafion film[12] and CNT-based films.[34,37] Thus, the GNS–Nafion composites improved the affinity of immobilized Hb to H_2O_2.

The reproducibility and stability of the biosensor were also investigated. The relative standard deviation was 3.1% for six determinations using a single-enzyme electrode at a H_2O_2 concentration of 1.0 μM. The fabrication of five electrodes, prepared under the same conditions independently, showed an acceptable reproducibility with a relative stand deviation of 3.4% for the currents determined at a H_2O_2 concentration of 1.0 μM. These results indicated that Hb immobilized in a GNS–Nafion composite film was an efficient and reproducible immobilization process. The stability of the biosensor was firstly tested by comparing the cyclic voltammetric peak currents of Hb. After continuously scanning for 100 cycles, the voltammetric response remained almost unchanged. The storage stability of the biosensor was investigated by testing every four days. When not in use, the biosensor was stored in 0.05 M pH 7.0 PBS at 4 °C. It retained 90% of its initial value after 3 weeks.

4. Conclusions

In this paper, for the first time, GNS–Nafion composites have been used to construct mediator-free biosensors. Due to good biocompatibility of the composite film, immobilized Hb retained its native structure. Hb immobilized in the composite film showed good direct electrochemistry and a fast electron-transfer rate. The electron-transfer rate constant k_s of Hb immobilized in the composite film was more than two times that of a CNF–Nafion composite film, and was more than one order of magnitude greater than most literature values for CNT-based films. The biosensor based on the direct electron transfer of the immobilized Hb showed good analytical performance, which was comparable or superior to the biosensors based on CNF- and CNTs-based biosensors. Moreover, the cheap cost of GNSs gives them more potential than CNTs and CNFs in the mass production of biosensors. Therefore, the GNS-based composite is a promising bio-immobilizing material, which can combine with various redox proteins and widely apply in mediator-free biosensors, bioelectronics and biofuel cells.

Acknowledgements

This work was supported by the National Natural Science Foundation of China (No. 20705004), the National 863 Project (No. 2006AAO3Z343), the 111 Project (No. B07004) and the Program for New Century Excellent Talents in University (Grant No. NCET-08-0713).

References

1 J. Wang, *Analyst*, 2005, **130**, 421–426.
2 X. Luo, A. Morrin, A. J. Killard and M. R. Smyth, *Electroanalysis*, 2006, **18**, 319–326.
3 I. Willner, R. Baron and B. Willner, *Biosens. Bioelectron.*, 2007, **22**, 1841–1852.
4 S. Sotiropoulou, V. Gavalas, V. Vamvakaki and N. A. Chaniotakis, *Biosens. Bioelectron.*, 2003, **18**, 211–215.
5 V. Vamvakaki and N. A. Chaniotakis, *Sens. Actuators, B*, 2007, **126**, 193–197.
6 A. Merkoci, M. Pumera, X. Llopis, B. Pérez, M. Valle and S. Alegret, *TrAC, Trends Anal. Chem.*, 2005, **24**, 826–838.
7 J. J. Gooding, *Electrochim. Acta*, 2005, **50**, 3049–3060.
8 G. A. Rivas, M. D. Rubianes, M. C. Rodríguez, N. F. Ferreyra, G. L. Luque, M. L. Pedano, S. A. Miscoria and C. Parrado, *Talanta*, 2007, **74**, 291–307.
9 V. Vamvakaki, K. Tsagaraki and N. Chaniotakis, *Anal. Chem.*, 2006, **78**, 5538–5542.
10 S. E. Baker, K. Y. Tse, C. S. Lee and R. J. Hamers, *Diamond Relat. Mater.*, 2006, **15**, 433–439.
11 N. Wu, X. Zhang and X. Ju, *Anal. Chem.*, 2007, **79**, 453–458.
12 X. Lu, J. Zhou, W. Lu, Q. Liu and J. Li, *Biosens. Bioelectron.*, 2008, **23**, 1236–1243.
13 H. Zhang, L. Fan and S. Yang, *Chem.–Eur. J.*, 2006, **12**, 7161–7166.
14 C. Petit, A. Gonzalez-Cortes and J. M. Kauffmann, *Talanta*, 1995, **42**, 1783–1789.
15 J. Wang, A. J. Reviejo and L. Angnes, *Electroanalysis*, 1993, **5**, 575–579.
16 Ü. A. Kirgöz, D. Odaci, S. Timur, A. Merkoci, S. Alegret, N. Besün and A. Telefoncu, *Anal. Chim. Acta*, 2006, **570**, 165–169.
17 G. Chen, W. Weng, D. Wu, C. Wu, J. Lu, P. Wang and X. Chen, *Carbon*, 2004, **42**, 753–759.

18 US Pat., 20 040 127 621, 2004.
19 W. N. Reynolds, *Physical properties of graphite*. Elsevier Publishing Co., Ltd.: NewYork, 1968.
20 T. R. Hendricks, J. Lu, L. T. Drzal and I. Lee, *Adv. Mater.*, 2008, **20**, 2008–2012.
21 T. Cassagneau and J. H. Fendler, *Adv. Mater.*, 1998, **10**, 877–881.
22 J. J. Mack, L. M. Viculis, A. Ali, R. Luoh, G. L. Yang, H. T. Hahn, F. K. Ko and R. B. Kaner, *Adv. Mater.*, 2005, **17**, 77–80.
23 A. Yu, P. Ramesh, M. E. Itkis, E. Bekyarova and R. C. Haddon, *J. Phys. Chem. C*, 2007, **111**, 7565–7569.
24 J. Lu, L. T. Drzal, R. M. Worden and I. Lee, *Chem. Mater.*, 2007, **19**, 6240–6246.
25 J. Lu, I. Do, L. T. Drzal, R. M. Worden and I. Lee, *ACS Nano*, 2008, **2**, 1825–1832.
26 C. Shan, H. Yang, J. Song, D. Han, A. Ivaska and L. Niu, *Anal. Chem.*, 2009, **81**, 2378–2382.
27 M. Zhou, Y. Zhai and S. Dong, *Anal. Chem.*, 2009, **81**, 5603–5613.
28 W. Zhang and G. Li, *Anal. Sci.*, 2004, **20**, 603–609.
29 M. Viticoli, A. Curulli, A. Cusma, S. Kaciulis, S. Nunziante, L. Pandolfi, F. Valentini and G. Padeletti, *Mater. Sci. Eng., C*, 2006, **26**, 947–951.
30 J. Wang, *Chem. Rev.*, 2008, **108**, 814–825.
31 L. Gorton, *Electroanalysis*, 1995, **7**, 23–45.
32 J. Wang, M. Musameh and Y. H. Lin, *J. Am. Chem. Soc.*, 2003, **125**, 2408–2409.
33 E. Laviron, *J. Electroanal. Chem.*, 1979, **101**, 19–28.
34 Y. D. Zhao, Y. H. Bi, W. D. Zhang and Q. M. Luo, *Talanta*, 2005, **65**, 489–494.
35 H. Qi, C. Zhang and X. Li, *Sens. Actuators, B*, 2006, **114**, 364–370.
36 R. Zhang, X. Wang and K. K. Shiu, *J. Colloid Interface Sci.*, 2007, **316**, 517–522.
37 C. Cai and J. Chen, *Anal. Biochem.*, 2004, **325**, 285–292.
38 C. E. Banks and R. G. Compton, *Analyst*, 2005, **130**, 1232–1239.
39 A. E. F. Nassar, Z. Zhang, N. Hu and J. F. Rusling, *J. Phys. Chem. B*, 1997, **101**, 2224–2231.
40 R. A. Kamin and G. S. Wilson, *Anal. Chem.*, 1980, **52**, 1198–1205.

